Aya MORITA[1], Fumiaki TAJIMA[2], Toshifumi YUJI[3], Sarizam MAMAT[4] and Narong MUNGKUNG[5]

Yokohama-yoshida Junior High School (1), Yokohama National University (2), University of Miyazaki (3)
Universiti Malaysia Kelantan (4), King Mongkut's University of Technology Thonburi (5)

Determination of the Complex Refractive Index of a Subwavelength-diameter Spider Thread on Silver Coating by Light Scattering

Abstract. *In this study, we have created nano-scale silver pipes by sputtering the silver material which frequently shows negative or less-than 1 refractive index onto the spider thread thinner than optical wavelength with. As a part of the study to investigate distribution of the complex refractive index which indicates optical and electromagnetic properties of the resulting silver pipes, we used light scattering method using linearly polarized laser with wavelength of 660 nm and radiated it perpendicularly to the silver pipe to measure the angular distribution of the scattered light intensity. Using the numerical calculation with Coaxial cylinder model based on the values found through preceding studies, we calculated the angular distribution of the scattered light intensity, and fitted the calculation result to the measurement result. This allowed us to determine the complex refractive index and outer diameter of the silver pipe along with the error range. The silver pipe was observed with field emission scanning electron microscope (FE-SEM) and the outer diameter of the silver pipe was estimated. This outer diameter was compared with the outer diameter obtained by fitting the calculation result with the light scattering method to the measurement result to evaluate the validity of the measurement result. This revealed that the result obtained with light scattering method has showed good agreement with that measured using FE-SEM.*

Streszczenie. *W artykule przedstawiono metodę badania nanorurek srebrnych wytwarzanych metodą rozpylania. Do badania właściwości rurek, przede wszystkim ich grubości wykorzystano pomiar światła rozproszonego na długości nici. Do pomiaru wykorzystano światło laserowe o o długości 660 nm. Opracowano model matematyczny metody pomiar współczynnika załamania światła. Dokładność metody potwierdzono wykorzystując mikroskop typu FE-SEM.* **Pomiar współczynnika załamania światła w srebrnej nanorurce metodą analizy rozpraszania światła laserowego**

Keywords: Light scattering, Silver, Spider thread, Complex refractive index, Coaxial cylinder model.
Słowa kluczowe: nanorurki srebrne, rozpraszanie świata, współczynnik załamania światła.

Introduction

The spider draglines are protein materials of natural structure with excellent mechanical properties. In the textile industry, they are presently expected to be used in transportation devices such as vehicles and airplanes, and electronic devices, or as suture thread for surgery or artificial blood vessel in medical field [1-4]. Certain spider draglines are known to be of strength comparable to iron and high-strength synthetic fibers. The strength of spider draglines can be of tensile strength of up to 1.6 GPa and Young's modulus of up to 10 GPa. It is known to be light yet strong and flexible [5-8]. Since spiders are carnivorous creatures and feed on each other, it is extremely difficult to breed spiders as done with domesticated silkworms. The disadvantage of spider draglines is that mass production of natural draglines is impossible [9]. While a bioprocess using microorganisms [10] has been suggested as an attempt to artificially synthesize draglines, it is not considered to be a suitable choice for mass production due to its low production efficiency and high cost. However, the materials smaller than light wavelength with mechanical, electrical, and optical properties comparable to those of nano-scale metal are expected to be used in plasmon [11-13] or metamaterial [14-17].

Since metallic materials (specially precious metals) showed different optical and electromagnetic properties at nano-scale level in the preceding studies, we deposited platinum and gold thin film on the spider thread and created nano-scale metallic pipes in a quest for possibility to realize materials with new functions [18]. As described in preceding studies, it is shown that understanding the complex refractive index, an indication for optical and electromagnetic properties, of the nano-scale metallic materials is critical to realize materials with new functions. However, previous studies on metallic pipes used expensive and rare precious metals and it may be difficult to apply the method in the industry. The complex refractive index of the precious metals is generally measured on a flat thin film with the thickness of about tens of mm. There are also studies on microparticles and there have been many data reported. But the complex refractive index of metallic materials thinner than light wavelength has not been sufficiently evaluated other than in the results of our research group.

In this study, we used silver, the most conductive and heat-conductive materials at room temperature among precious metals, to be deposited on the spider draglines through sputtering to create nano-scale silver pipes. In order to evaluate the complex refractive index and its distribution that will indicate the optical and electromagnetic properties of the silver pipe created, we radiated linearly polarized laser perpendicularly to the silver pipe and measured the angular distribution of the scattered light intensity. Using the values obtained in the angular distribution of the scattered light intensity measured, and the values of the angular distribution of the scattered light intensity obtained through numerical calculation with Coaxial cylinder model [19], we realized to find the complex refractive index and outer diameter of the silver pipe created by sputter-depositing the silver with light-scattering method.

Model and calculated scattering intensity

Fig. 1 shows the overview of the Coaxial cylinder model with which numerical calculation of the angular distribution of the scattered light intensity of the silver pipe was made. In this study, we made numerical calculations based on the Coaxial cylinder model. In the figure, r_1 and n_1 represent the radius and refractive index respectively of the dragline, and r_2 and $\tilde{n}_2$ the radius and complex refractive index of the silver pipe. The incident waves $E_\perp$ and $E_\parallel$ indicate that the electric field E of the respective wave is parallel or perpendicular to the axis z. With perpendicular polarization $E_\perp$ that enters the cylinder perpendicularly, the differential cross section of the scatter pattern of parallel polarization $E_\parallel$ or $\sigma_{\parallel,\perp}(\theta_{sc})$ can be expressed as in the equation (1).
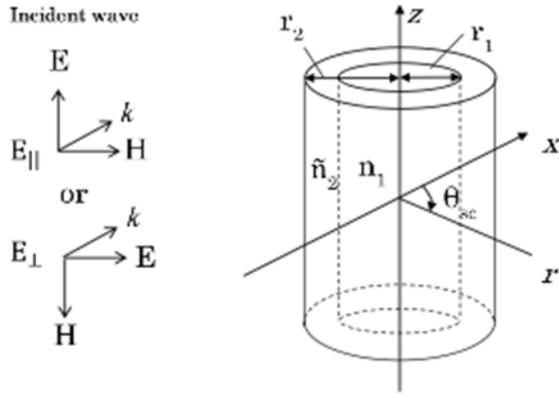
Fig.1. Schematic diagram of Ag pipe and coordinate axes.

(1)

$$\sigma_{\|,\perp}(\theta_{sc}) = \frac{2}{\pi k} \left| \sum_{m=0}^{\infty} B(m)_{\|,\perp} \cos(m\theta_{sc}) \right|^2$$

Where θ_{sc} is the scattering angle and

(2)

$$B(m)_{\|,\perp} = \frac{-J'_m(kr_2)c_1(m)_{\|,\perp} - J_m(kr_2)c_2(m)_{\|,\perp}}{H_m^{(1)'}(kr_2)c_1(m)_{\|,\perp} - H_m^{(1)}(kr_2)c_2(m)_{\|,\perp}}$$

$$\times (2 - \delta_{m0})$$

Here, for wave $E_{\|}$,

(3)

$$\begin{pmatrix} c_1(m)_{\|} \\ c_2(m)_{\|} \end{pmatrix} = \begin{pmatrix} H_m^{(1)}(\tilde{n}_{2\|}kr_2) & H_m^{(2)}(\tilde{n}_{2\|}kr_2) \\ \tilde{n}_{2\|}H_m^{(1)'}(\tilde{n}_{2\|}kr_2) & \tilde{n}_{2\|}H_m^{(2)'}(\tilde{n}_{2\|}kr_2) \end{pmatrix}$$

$$\times \begin{pmatrix} \tilde{n}_{2\|}H_m^{(2)'}(\tilde{n}_{2\|}kr_1) & -H_m^{(2)}(\tilde{n}_{2\|}kr_1) \\ -\tilde{n}_{2\|}H_m^{(1)'}(\tilde{n}_{2\|}kr_1) & H_m^{(1)}(\tilde{n}_{2\|}kr_1) \end{pmatrix} \times \begin{pmatrix} J_m(n_{1\|}kr_1) \\ n_{1\|}J'_m(n_{1\|}kr_1) \end{pmatrix}$$

For wave $E_{\perp}$

(4)

$$\begin{pmatrix} c_1(m) \\ c_2(m) \end{pmatrix}_{\perp} = \begin{pmatrix} H_m^{(1)}(\tilde{n}_{2\perp}kr_2) & H_m^{(2)}(\tilde{n}_{2\perp}kr_2) \\ \dfrac{H_m^{(1)'}(\tilde{n}_{2\perp}kr_2)}{\tilde{n}_{2\perp}} & \dfrac{H_m^{(2)'}(\tilde{n}_{2\perp}kr_2)}{\tilde{n}_{2\perp}} \end{pmatrix}$$

$$\times \begin{pmatrix} \dfrac{H_m^{(2)}(\tilde{n}_{2\perp}kr_1)}{\tilde{n}_{2\perp}} & -H_m^{(2)}(\tilde{n}_{2\perp}kr_1) \\ \dfrac{-H_m^{(1)'}(\tilde{n}_{2\perp}kr_1)}{\tilde{n}_{2\perp}} & H_m^{(1)}(\tilde{n}_{2\perp}kr_1) \end{pmatrix} \times \begin{pmatrix} J_m(n_{1\perp}kr_1) \\ J'_m(n_{1\perp}kr_1)/n_{1\perp} \end{pmatrix}$$

Where J_m is the Bessel function of the first kind of the size m, and $H_m^{(1)}$ is the Hankel function with wavenumber $k=2\pi/\lambda$. The δ indicates Kronecker delta, and prime indicates differentiation. For $E_{\perp}$, the coefficients n_1 and $\tilde{n}_2$ not included in the arguments of Bessel function and Hankel function are replaced with $1/n_{1\perp}$ and $1/\tilde{n}_{2\perp}$ respectively. However, $n_{1\perp}$ and $\tilde{n}_{2\perp}$ are refractive index and complex refractive index respectively for perpendicular polarization $E_{\perp}$, and ultimately, the complex refractive index will be $n=n_{1\|}+n_{2\|}$ i, where n_1 is the real part and n_2 the imaginary part. In case of perpendicular polarization, $\|$ is replaced with $\perp$. The dielectric constant ε_0 inside the pipe

is assumed to be the one in vacuum and uniaxially anisotropic, and expressed with the equation (5).

(5)

$$\varepsilon_0 \begin{bmatrix} n_{1\perp}^2 & 0 & 0 \\ 0 & n_{1\perp}^2 & 0 \\ 0 & 0 & n_{1\|}^2 \end{bmatrix}$$

The parameters such as outer diameter and complex refractive index of the silver pipe are determined through fitting so that the deviation index in the equation (6) will be the lowest, where I_i and σ_i (= $\sigma_{i\|}$ or $\sigma_{i\perp}$) indicate the measured scattered light intensity and the value calculated with equation (1) respectively with measured scattering angle $\theta_{sc} = \theta_i$.

(6)

$$U_1(n_1, \tilde{n}_2, r_{1,2}) = \frac{\sum_i \left[I_i - I_0\sigma_i(n_1, \tilde{n}_2, r_{1,2}) \right]^2}{\sum_i I_i}$$

When the calculated angular distribution of the scattered light intensity of the silver pipe is most close to the pattern of the measured data (when the "uncertainty index" is the lowest), the refractive index $\tilde{n}$ and outer diameter D are determined to be optimum. The "uncertainty index" is calculated by the method of least squares [20].

Experimental and setup

Fig. 2 shows the overview of how we measured the angular distribution of the scattered light intensity. A single dragline of a tetragnatha praedonia [21] (Body size: 1.0 – 2.0 mm)is dropped from the top to be collected into the sample storage holder and its thickness ($2r_1$) and the radius of the inner diameter (n_1) are to be determined in advance [18]. Next, the dragline will be sputter-deposited with a thin silver film using magnetron sputtering method in the compact sputtering system (Quick Cool Coater SC-701MC ; Sanyu Electron Co., Ltd.), and the angular distribution of the scattered light intensity is measured. The laser with wavelength of 660 nm was irradiated perpendicularly to the sample (Non-coated) in a dark room, and the scattered light intensity around was measured for every 4.0 degrees of the scattering angle. The scattering angle is 0 degree in the laser forwarding direction, and was measured after excluding the angle in shadow （−6.0 degree ～−50 degree or −134 degree ～147 degree or 6.0～162 degree） . When the laser was irradiated perpendicularly to the z axis of the silver pipe, the intensity of the scattered light was measured with the scattering angle θ_{sc} and at the distance r sufficiently far. By fitting the angular distribution of the scattered light intensity through numerical calculation from the Coaxial cylinder model to the angular distribution of the scattered light intensity obtained through measurement, we determined the outer diameter ($2r_2$) and complex refractive index ($\tilde{n}_2$) of the silver pipe. After measuring the angular distribution of the scattered light intensity, we used FE-SEM (JSM-7001F ; JEOL) to observe the surface of the silver pipe and measured its outer diameter. We verified the validity of the outer diameter of the silver pipe found from the complex refractive index using the light scattering method by fitting the angular distribution of the scattered light intensity found through numerical calculation using the Coaxial cylinder model to the measured angular distribution of the scattered light intensity, and the outer diameter measured with FE-SEM.
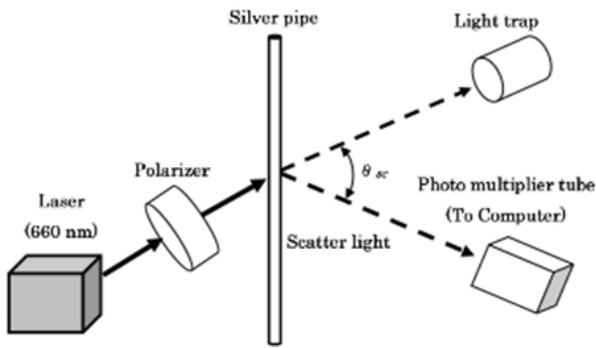
Fig.2. Experimental setup of measuring devices.

Results and discussion

Figure 3 shows the measurement result of the angular distribution of the scattered light intensity of the dragline before sputtering. From the figure, we can see that the measured values of the angular distribution of the scattered light intensity and the values found through numerical calculation mostly agree. Assuming that the circularity of the dragline at this point will affect the measurement result of the diameter of the dragline (error range), almost no difference was observed in the measurement result, and thus it was revealed that the dragline was almost a true circle. Where $\theta_{sc} < 0$ in the figure, the data is missing because the dragline was collected into the sample storage holder, and the area was in the shadow of the sample storage holder and could not be measured.

Figure 4 shows the measurement result of the angular distribution of the scattered light intensity of the silver pipe. The (a) in the figure is the measurement result at about 1.0 mm below the center of the silver pipe, and (b) at about 1.0 mm above the center. The same pipe was used for both conditions. From those figures, we can confirm that the measured values in the angular distribution of the scattered light intensity and the values found through numerical calculation mostly agree.
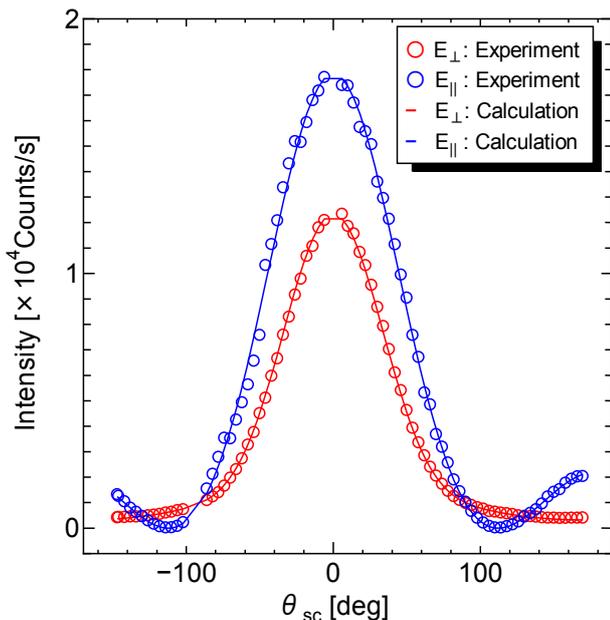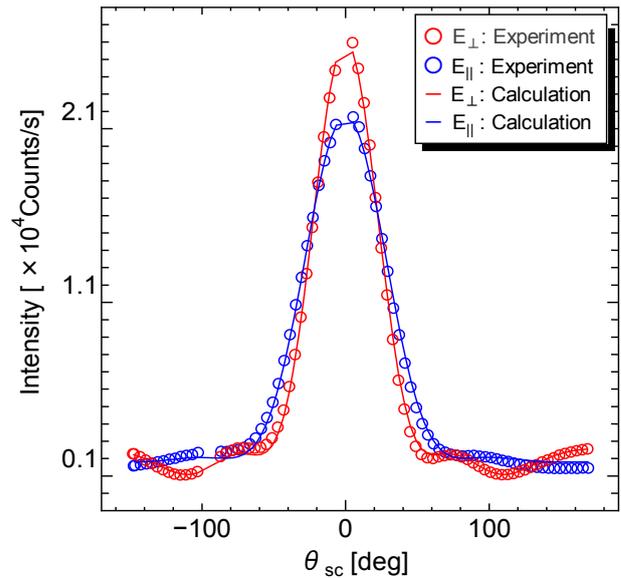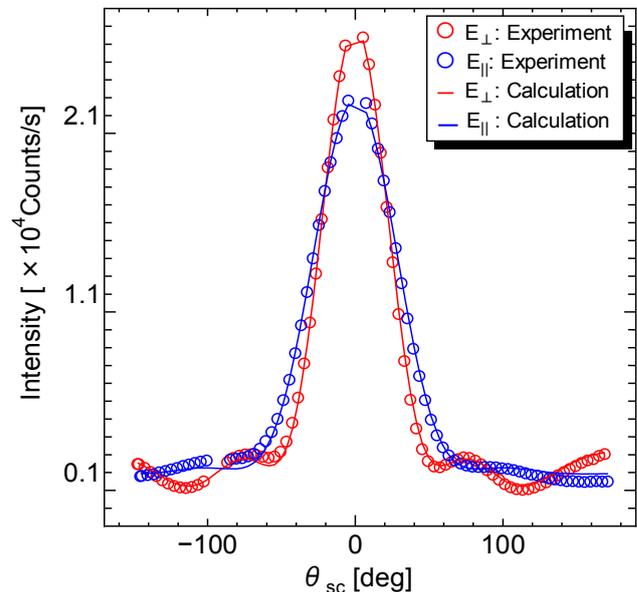

(a) 1.0 mm below the center

(b) 1.0 mm above the center

Fig.2. Angular distributions of scattered light intensity of silver pipes. Circles and solid curves show measured data and theoretical calculations, respectively. Expressions $E_{\parallel}$(blue) and $E_{\perp}$ (Red) are respectively the corresponding parallel and perpendicularly polarized incident waves.

Table 1 summarizes the complex refractive index of the silver pipe obtained through light scattering method that fits the values in the angular distribution of the scattered light intensity found through numerical calculation using the Coaxial cylinder model in Fig. 4 to the values in the angular distribution of the measured scattered light intensity. Here, we assumed $D_1 = 2r_1$ and $D_2 = 2r_2$. Considering the fact that from the preceding studies, the optimum parameters such as complex refractive index is determined uniquely when $E_{\perp}$ but often not when $E_{\parallel}$, we assumed $r_{2\parallel} = r_{2\perp}$ to determine $\tilde{n}_2$ when $E_{\parallel}$. For this reason, there is no uncertainty range given for r_2 when $E_{\parallel}$. The error of U_1 in the figure (a) and (b) is approximately 5.0 % and the values almost agree. They almost agree for n_1, D_1, and $\tilde{n}_2$ as well. However, the outer diameter D_2 was fixed to the value determined when $E_{\perp}$ but only for when $E_{\parallel}$. With $E_{\perp}$ and $E_{\parallel}$ in the figure (a), the outer

Fig.3. Angular distributions of scattered light intensity of non-coated spider thread.

diameter D_2 of the silver pipe was calculated to be 475 nm. Similarly, with $E_\perp$ and $E_\parallel$ in the figure (b), the outer diameter D_2 of the silver pipe was calculated to be 460 nm. Comparing the outer diameter D_2 of the silver pipe in the figure (a) and (b), we confirmed the error to be 5.0 %.

Fig. 5 shows the image of the silver pipe observed with FE-SEM. From the figure, we can estimate the outer diameter of the silver pipe to be about 445 nm. This is quite close to 460 nm to 475 nm, the outer diameter found from the complex refractive index of the silver pipe obtained from light scattering, and almost agrees with the outer diameter of the silver pipe found with the light scattering method. Thus, it was revealed that the outer diameter D_2 of the silver pipe found from the light scattering method almost agrees with the outer diameter actually measured.

Table 1. Optimum parameters for silver fibers (Sample (a) and Sample (b)).

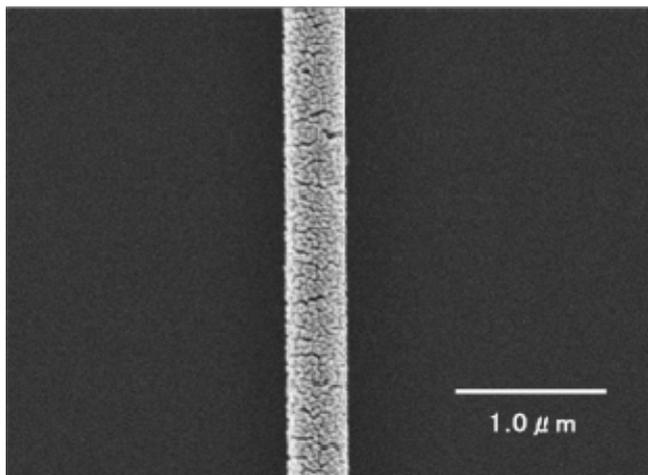| Sample	n/r	$E_\perp$	$E_\parallel$
(a)	n_1	$1.576^{+0.044}_{-0.048}$	$1.648^{+0.222}_{-0.248}$
	D_1(nm)	336^{+15}_{-16}	338^{+31}_{-23}
	$\tilde{n}_2$	$1.71^{+0.40}_{-0.31}+1.01^{+0.28}_{-0.41}\,i$	$1.51^{+0.21}_{-0.19}+1.06^{+0.25}_{-0.29}\,i$
	D_2(nm)	475^{+35}_{-35}	475
	U(%)	5.2	5.4
(b)	n_1	$1.576^{+0.044}_{-0.048}$	$1.648^{+0.222}_{-0.248}$
	D_1(nm)	336^{+15}_{-16}	338^{+31}_{-23}
	$\tilde{n}_2$	$1.61^{+0.30}_{-0.29}+1.31^{+0.16}_{-0.20}\,i$	$1.66^{+0.31}_{-0.24}+1.21^{+0.30}_{-0.31}\,i$
	D_2(nm)	460^{+20}_{-18}	460
	U(%)	4.6	5.5

Fig.5. Photograph of FE-SEM image of silver pipe.

Conclusion

In this study, we sputter-deposited silver material onto the spider dragline which is thinner than the light wavelength to create a nano-scale silver pipe. In order to find the distribution of the complex refractive index that will indicate optical and electromagnetic properties of the silver pipe created, we used the light scattering method and irradiated linearly polarized laser with wavelength of 660 nm perpendicularly to the silver pipe to measure the angular distribution of the scattered light intensity. We also used the A model to fit the angular distribution of the scattered light intensity found through numerical calculation to the angular distribution of the scattered light intensity obtained to try to calculate the complex refractive index and the outer diameter of the silver pipe. The result revealed the followings.

(1) The measurement of the angular distribution of the scattered light intensity of the spider dragline before sputtering revealed that the measured angular distribution of the scattered light intensity and the calculated angular distribution found through numerical calculation mostly agreed. The spider dragline was measured before coating, and this result validates that its circularity was quite a true circle.

(2) Through light scattering method which fits the angular distribution of the scattered light intensity found through numerical calculation with the Coaxial cylinder model to the measured angular distribution of the scattered light intensity, the value U_1 with $E_\perp$ and $E_\parallel$ found from the complex refractive index of the silver pipe obtained showed about the same error of around 5.0 %. Similarly, n_1 and D, and $\tilde{n}_2$ also showed agreeing values.

(3) Through light scattering method which fits the angular distribution of the scattered light intensity found through numerical calculation with the Coaxial cylinder model to the measured angular distribution of the scattered light intensity, the outer diameter of the silver pipe found from the complex refractive index of the silver pipe obtained was calculated to be 460 nm to 475 nm. The values of the outer diameter of the silver pipe calculated were almost the same when $E_\perp$ and $E_\parallel$ as well.

(4) The observation of the outer diameter of the silver pipe with FE-SEM gave us an estimated outer diameter of the silver pipe to be approximately 445 nm. This revealed to be almost the same as the outer diameter of the silver pipe obtained with light scattering method.

In the future, we are going to create metallic pipes by sputtering different metallic materials onto the spider thread and investigate the distribution of the complex refractive index to find out the properties of the metallic pipes. Along with that, we are also going to investigate the dependency of the complex refractive index on shape, etc. to evaluate the application of the metallic pipes using the spider thread in various industrial use.

Authors: *Miss. Aya MORITA, Yokohama-Yoshida Junior High School, 1-1, Gakuenkibanadai-nishi, Miyazaki, 889192, Japan, E-mail: moritaaya6211@gmail.com; Emiritus Prof. Fumiaki TAJIMA, Yokohama National University, Tokiwadai, Hodogaya-ku,Yokohama, 2408501, Japan, E-mail: tajima@ynu.ac.jp; dr. Toshifumi YUJI, Faculty of Education, University of Miyazaki, 1-1, Gakuenkibanadai-nishi, Miyazaki, 889192, Japan, E-mail: yuji@cc.miyazaki-u.ac.jp; dr. Sarizam MAMAT, Advanced Materials Research Cluster, Faculty of Bioengineering and Technology, University Malaysia Kelantan, 17600, Jeli, Kelantan, Malaysia, E-mail: sarizam@umk.edu.my; dr. Narong MUNGKUNG, Department of Electrical Technology Education, King Mongkut's University of Technology Thonburi, 126 Pracha Uthit Rd, Bang Mot, Thung Khru, Bangkok, 10140, Thailand, E-mail: narong_kmutt@hotmail.com;*

REFERENCES
[1] Rising A., "Controlled assembly: A prerequisite for the use of recombinant spider silk in regenerative medicine?". *Acta Biomater*. 10(4) (2014),1627-1631.
[2] Ko F. K. and Jovicic J., "Modeling of mechanical properties and structural design of spider web". *Biomacromolecules*. 5(3) (2004), 780–785.
[3] Li X., Zong L., Wu X., You J., Li M. and Li C., "Biomimetic engineering of spider silk fibres with graphene for electric devices with humidity and motion sensitivity". *J. Mater. Chem. C*. 6(2018), 3212–3219.
[4] Lin C. B., Lee Y.-T. and Liu C.-Y., "Optimal photonic nanojet beam shaping by mesoscale dielectric dome lens". Journal of Applied Physics. 127 (2020), 243110.
[5] Omenetto F. G and Kaplan D L., "A new route for silk". *Nat. Photonics*. 2008; 2: 641–643.
[6] Zheng Y., Bai H., Huang Z., Tian X., Nie F. Q., Zhao Y., Zhai J. and Jiang L., "Directional water collection on wetted spider silk". *Nature*. 463 (2010), 640–643.

[7] Hayashi C. Y., Shipley N. H. and Lewis R. V., "Hypotheses that correlate the sequence, structure, and mechanical properties of spider silk proteins". *Int. J. Biol. Macromol*. 24 (1999), 271-275.

[8] Hinman M. B., Jones J. A. and Lewis R. V., "Synthetic spider silk: a modular fiber, *Trends Biotechnol*., 18 (2000), 374-379.

[9] Andersson M., Jia Q., Abella A., Lee X. -Y., Landreh M., Purhonen P., Hebert H., Tenje M., Robinson C. V, Meng Q., Plaza G. R., Johansson J. and Rising A., "Biomimetic spinning of artificial spider silk from a chimeric minispidroin", *Nat Chem Biol*. 13(3) (2017), 262-264.

[10] Tsuchiya K. and Numata K., "Chemical synthesis of multiblock copolypeptides inspired by spider dragline silk proteins", *ACS Macro Lett*., 6(2) (2017), 103-106.

[11] Mayer K. M. and Hafner J. H., "Localized surface plasmon resonance sensors"., *Chem. Rev*., 111(6) (2011), 3828–3857.

[12] Zhang S., Fan W., Panoiu N. C., Malloy K. J., Osgood R. M. and Brueck S. R. J., "Experimental demonstration of near-infrared negative-index materials", *Phys. Rev. Lett*., 95 (2005) 137404.

[13] Homola J. Y. S. and Gauglitz G., "Surface plasmon resonance sensors: review", *Sensors and Actuators B:Chemical*., 54 (1-2) (1999), 3–15.

[14] Smith D. R., Padilla W. J., Vier D. C., "Nemat-Nasser S. C. and Schultz S., Composite Medium with Simultaneously negative permeability and permittivity". *Phys. Rev. Lett*., 84(18) (2000), 4184-4187.

[15] Padilla W. J., Basov D. N. and Smith D. R., "Negative refractive index metamaterials", *Materials Today*., 9(7–8) (2006), 28–35.

[16] Hajian H, Ghobadi A, Butun B and Ozbay E, "Active metamaterial nearly perfect light absorbers: a review", *J. Opt. Soc. Am. B*., 36(8) (2019), F131-F143.

[17] Shalaev V. M., "Optical negative-index metamaterials", *Nature Photonics*., 1 (2007), 41–48.

[18] Tajima F. and Nishiyama Y., "Determination of the complex refractive index of a subwavelength-diameter platinum or gold pipe by light scattering", *J. Opt. Soc. Am*. A33(9) (2016), 1654-1660.

[19] Tajima F. and Nishiyama Y., "Light scattering from a birefringent cylinder, spider silk, slimmer than the wavelength approaches dipole radiation", *J. Opt. Soc. Am*. A22(6) (2005), 1127-1131.

[20] Tajima F., Nishiyama Y., Hiroi N. and Hashimoto Y., "Determination of the complex refractive index of a subwavelength-diameter platinum or gold pipe by light scattering", *J. Opt. Soc. Am*. A27(1) (2010), 1-5.

[20] Yuan L., Zhao L. J. and Zhang Z. S., "Preliminary study on the spider diversity of the wanglang national nature reserve. ", *Acta Arachnologica Sinica*., 2019; 28(1):7-36.